Journal of proteome research

pubs.acs.org/jpr

Article

Pilot Study of Metabolomic Biomarkers Associated with Outcomes in Patients with Lung Cancer Undergoing Radiation Therapy

Wei Meng,[‖] Rui Xu,[‖] Eric Miller, Xiaowei Sun, Jennifer Thurmond, Amy Webb, Joseph McElroy, Joshua Palmer, Dominic J. DiCostanzo, Shiqi Zhang, Hisashi Yamaguchi, Saikh Jaharul Haque, Jiangjiang Zhu,* and Arnab Chakravarti*

Cite This: *J. Proteome Res.* 2025, 24, 1662−1671

Read Online

ACCESS | Metrics & More | Article Recommendations | Supporting Information

ABSTRACT: Lung cancer stands as the leading cause of cancer-related death worldwide, impacting both men and women in the United States and beyond. Radiation therapy (RT) serves as a key treatment modality for various lung malignancies. Our study aims to systematically assess the prognosis and influence of RT on metabolic reprogramming in patients diagnosed with nonsmall-cell lung cancer (NSCLC) through longitudinal metabolic profiling. A cohort of 54 NSCLC patients underwent thoracic radiotherapy, with 96% receiving a total radiation dose ranging from 40 to 70 Gy, averaging 56.3 Gy. Blood biospecimens were collected before RT, during RT, and at the first follow-up after RT, with a total of 126 serum samples randomized for liquid chromatography−mass spectrometry (LC−MS) metabolomics analysis using a high-performance LC (HPLC)-Q-Exactive mass spectrometry system. Our results indicated that the serum metabolite coumarin derivatives prior to radiotherapy exhibited the strongest unfavorable outcome with overall survival in these NSCLC cases. The metabolites in the blood samples can reflect the responses during RT. Notably, over half of the metabolites (12/23) were found to be fatty acids in the longitudinal analysis. This pilot study indicated that metabolic profiling of biofluids from NSCLC patients undergoing RT has the potential to assess the patient outcomes during and after treatment.

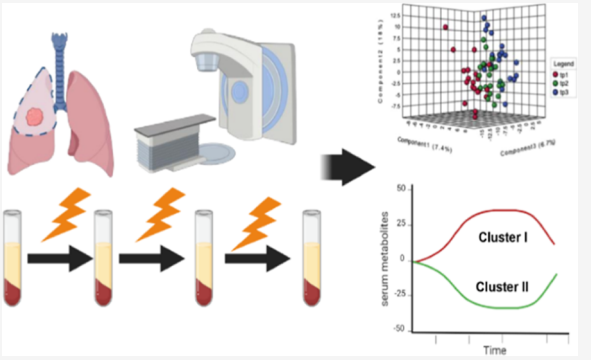

KEYWORDS: *metabolomics, lung cancer, metastasis, radiation treatment*

INTRODUCTION

Lung cancer remains the most common cause of cancer-related death for both men and women in the United States and around the world.[1,2] Currently, lung cancer research largely focuses on anticancer therapies for non-small cell lung cancer (NSCLC), which accounts for 85% of all lung cancer cases.[3,4] While surgical resection of early stage NSCLC remains the standard of care in eligible patients, radiation therapy (RT) plays a central role in patients ineligible for surgical resection or in patients with more advanced disease.[5−7] In order to achieve a high tumor control rate of lung malignancies, thoracic radiation therapy with concurrent chemotherapy is unavoidably associated with the risk of radiation-induced pulmonary complications.[8] The advancement of stereotactic body radiation therapy (SBRT) or stereotactic ablative radiotherapy (SABR) has revolutionized the management of early-stage NSCLC.[9]

Metabolic reprogramming, a hallmark of cancer cells, has been a focus of cancer biology research since Otto Warburg discovered upregulated glycolysis in cancer cells in 1927.[10,11] Recent advances in high-throughput studies revealed that genome-wide alterations exist in different biological layers of cancer cells and surrounding normal cells, providing opportunities for the discovery and development of potential targeted therapeutic agents. Liquid chromatography linked to tandem mass spectrometry (LC−MS/MS) takes a central role in metabolism studies because it can assess a large number of small biological molecules in patient samples both quantitatively and simultaneously. Reprogramming of metabolism in tumor cells and tumor-associated microenvironments not only provides the required energy and metabolites to support tumor growth but also mediates the resistance of tumor cells to antitumor therapies. This reprogramming of metabolism not only sustains tumor growth but also mediates resistance to antitumor therapies. Metabolomic biomarkers hold the potential for assessing radiation response and resistance simultaneously, informing treatment modulation, and serving as prognostic markers for cancer patient outcomes. A recent

Received: July 18, 2024
Revised: November 26, 2024
Accepted: December 20, 2024
Published: March 12, 2025

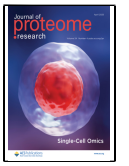

https://doi.org/10.1021/acs.jproteome.4c00529
J. Proteome Res. 2025, 24, 1662−1671

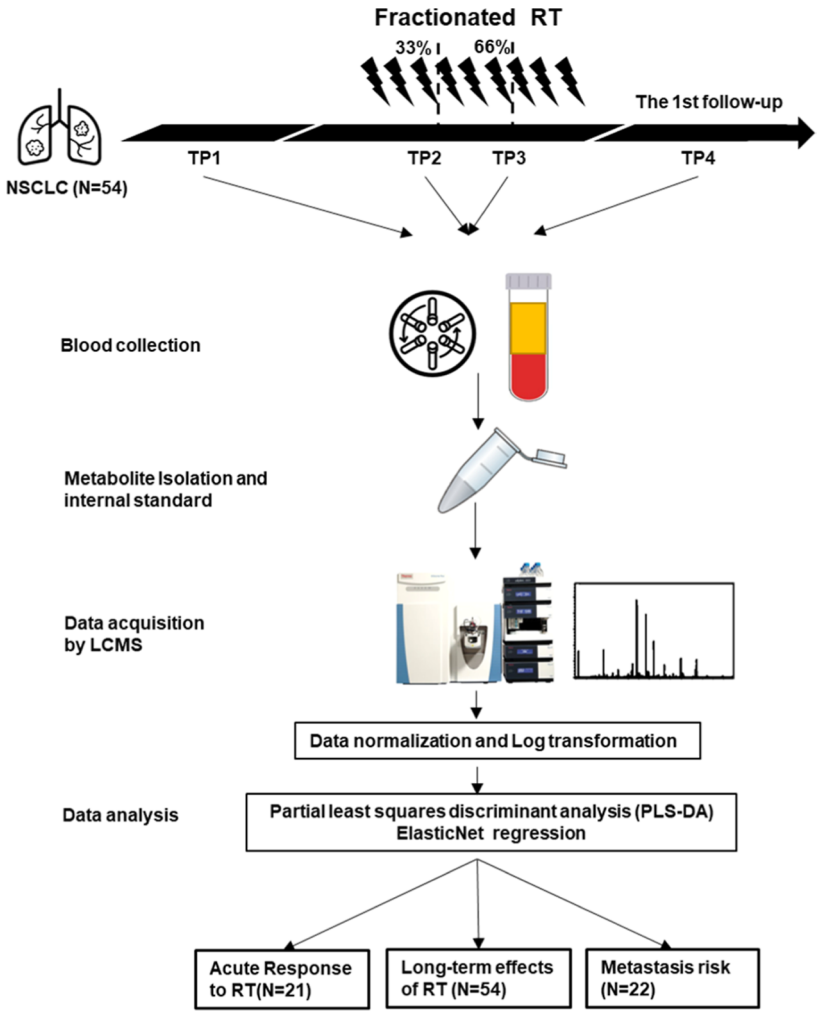

Figure 1. Schematic workflow demonstrating the study methods.

report indicates that plasma amino acid levels in NSCLC patients are significantly altered compared to controls.[12] A second metabolome study investigating pelvic radiation therapy for patients with high-risk prostate cancer indicates that the metabolic profiles of plasma and stool samples can reflect the molecular changes during radiation therapy.[13]

Metabolomics, offering insights into the metabolic landscape of tumors and surrounding tissues, holds promise as a prognostic tool in lung cancer. However, its role in assessing radiotherapy treatment outcomes for NSCLC patients has yet to be fully established. In this pilot study, we aimed to systematically evaluate both the prognostic value and treatment response of metabolomics in lung cancer patients undergoing radiotherapy. We hypothesized that specific small molecules in patients' biofluids could serve as indicators, reflecting the association between metabolic profiles and radiation response during the course of radiation treatment.

EXPERIMENTAL SECTION

Study Design

Fifty-four lung cancer patients (26 cases of adenocarcinoma, 21 cases of squamous cell carcinoma, 4 cases of adenosquamous carcinoma, and 3 cases of large cell carcinoma in Table S1) were consented prior to the start of radiation treatment between 2012 and 2016. Blood biospecimens were collected at several time points before, during, and follow-up care after radiation treatment. The time points for the biospecimen collections were set as follows: TP1—before radiation treatment, TP2—biospecimen collection occurred after completion of the first third of the treatment, TP3—biospecimen collection occurred after completion of the second third of the treatment, and TP4—biospecimens were collected when patients returned for their follow-up visit at the Radiation Oncology department (1−3 months following completion of treatment). The thoracic radiotherapy regimen included a range of 3 to 48 fractions, with a median of 30 fractions. Each fraction ranged from 1.25 to 17 Gy, with a median of 2 Gy per fraction. Additionally, the median biological effective dose, calculated using the linear-quadratic model with an alpha-beta ratio of 10 Gy, ranged from 37.5 to 137.7 Gy, with a median of 74.3 Gy (Supporting Information Table 1).

The blood samples were collected in the red top collection tube, and the liquid fractions were isolated by centrifugation at 1000*g* for 10 min. Then, the serum samples were stored in cryogenic tubes at −80 °C until subjected to analysis. An institutional review board (IRB) approved the research protocol (2011C0038). An overview of the workflow of the study is shown in Figure 1.

https://doi.org/10.1021/acs.jproteome.4c00529
J. Proteome Res. 2025, 24, 1662−1671

Serum Sample Preparation and High-Performance Liquid Chromatography–Mass Spectrometry Metabolite Profiling

The serum sample preparation method has been reported in our previously published studies, and the details are provided in the Supporting Information, together with the detailed high-performance LC (HPLC)–MS setup.[14] Briefly, LC–MS analysis was performed to analyze the prepared serum samples on an HPLC-Q-Exactive mass spectrometer system with an XBridge BEH Amide XP column (130 Å, 2.5 μm, 2.1 mm × 150 mm, 2.5 μm particle size; Waters Corporation, Milford, MA). Given that the longitudinal serum samples were acquired over several years, all of the samples were randomized and analyzed by LC–MS together to avoid batch effects. Additionally, to correct for the instrument variability during the data normalization process, a panel of internal standards was spiked into the serum samples, and commercially available human serum samples were used for quality control during the data acquisition (Table S2 and Figure S1).

The Thermo Scientific Compound Discoverer 3.1 package was used to extract features and identify metabolites from raw spectra using both online and local databases, including mzCloud,[15] Metabolika,[16] ChemSpider,[17] predicted compositions, and a local mass list of 167 standard compounds.[18] The representative serum metabolic features of NSCLC patients from our study are demonstrated in Figure S2. Research data are stored in an institutional repository and will be shared upon request with the corresponding author.

Statistical Analyses

Based on the collection stages (TP1–TP4) and clinical status [no metastasis (Mets), brain Mets, and other Mets], these samples were labeled and analyzed by the partial least squares discriminant analysis (PLS-DA) to observe metabolic differences. In the subgroup analysis, a heatmap and PLS-DA model were used to classify data from different time points, and the volcano plot was applied to select the significant metabolites. In the paired analysis at the four time points, variable importance projection (VIP) > 0.8 and p-value < 0.05 were used to distinguish the differential metabolites. The area under the curve (AUC) of PLS-DA results was used to evaluate the overall metabolic changes of metabolic pathways. A p-value < 0.05 was considered a significant difference in the pairwise comparison between time points. To evaluate the predisposed risks of metastasis in patients, the ElasticNet prediction model was adopted to investigate the incidence of tumor metastasis.[19] In this study, $\alpha = 0.5$ was selected, assigning equal weight to ridge regression and least absolute shrinkage and selection operator (LASSO) regression.[20] To study the impact of radiation treatment on metabolic phenotypes, we performed the analysis including only TP1 and all TPs in patients with nonmetastatic and metastatic NSCLC.

RESULTS AND DISCUSSION

Clinical and Demographic Features of Study Participants

Fifty-four lung NSCLC patients were enrolled from October 5, 2012, to 28, 2015 (Table 1), and received either conventional or hypofractionated IMRT radiation therapy. The median age at the time of diagnosis was 66 years (range 60.0–76.8 years; Table 1). In 9 of the 54 cases, brain metastases were present, and in 13 of the 54 cases, metastatic disease but not brain metastasis was present (Tables 1 and S1). The patients who developed brain metastases displayed poorer overall survival compared with those without brain metastases (data not shown), emphasizing the need for a large cohort size to validate the statistical significance in the future.

Table 1. Demographic Information

	number of patients (%)
Age at Diagnosis	
median	66
IQR	60.0–76.8
Race	
white	49 (90.7)
black	2 (3.7)
Asian	1 (1.9)
other	2 (3.7)
Gender	
male	29 (53.7)
female	25 (46.3)
Initial AJCC Stage	
IA	11 (20.4)
IB	5 (9.3)
IIA	2 (3.7)
IIB	7 (13.0)
IIIA	12 (22.2)
IIIB	6 (11.1)
IV	11 (20.4)
Lung Histology	
adenocarcinoma	26 (48.1)
squamous cell carcinoma	21 (38.9)
adenosquamous carcinoma	4 (7.4)
other	3 (5.6)
Metastases Status	
no metastatic disease	32 (59.3)
metastatic disease w/o brain metastasis	13 (24.0)
brain metastasis	9 (16.7)

Serum Biomarkers Predicting Overall Survival and Metastatic Status in Lung Cancer Patients Prior to Radiotherapy

We performed Cox regression analyses in patients with pretreatment serum samples by median stratification of metabolite levels, and 19 metabolites were found to be significantly associated with overall survival. Coumarin, a blood thinner, was the identified serum metabolite, showing the strongest inverse correlation with overall survival (Table 2). Although anticoagulant therapy alleviates comorbidity conditions such as pulmonary embolism and venous thrombosis, it does not enhance the prognosis for individuals with lung cancer from a recent meta-analysis.[21,22] Our result supports this observation. The additional metabolites associated with patient outcomes predominantly belong to *N*-glycan biosynthesis, purine metabolism, and taurine metabolism. These dysregulated metabolic pathways are potentially linked to lung cancer pathogenesis and influence responses to radiation treatment. We also applied the ElasticNet machine learning model to our metabolomics data set. In total, the ElasticNet model identified 25 metabolites predicting the occurrence of metastasis (including brain and other organs) in the serum samples before radiation treatment (Table S4). Validating this list of metabolites and their corresponding coefficients in a large lung cancer cohort will be crucial for demonstrating robustness in the future.[24,25]

https://doi.org/10.1021/acs.jproteome.4c00529
J. Proteome Res. 2025, 24, 1662–1671

Table 2. Cox Regression Analysis Assesses Overall Survival in Relation to Serum Metabolites Prior to Radiotherapy

	Cox-model N = 47	
metabolite	HR (95% CI)	p value
coumarin	0.36 (0.18−0.7)	6.67×10^{-4}
taurine	0.4 (0.21−0.79)	3.70×10^{-3}
$C_{18}H_{34}O_4$	0.44 (0.23−0.84)	9.03×10^{-3}
hypoxanthin	0.45 (0.23−0.87)	1.01×10^{-2}
pseudoecgonine	0.45 (0.23−0.89)	1.02×10^{-2}
N_8-acetylspermidine	0.45 (0.23−0.88)	1.14×10^{-2}
3,26-dihydroxyfurost-20(22)-en-12-one	2.21 (1.13−4.3)	1.14×10^{-2}
2-amino-4-methylpyrimidine	0.46 (0.24−0.88)	1.26×10^{-2}
hexamethylenetetramine	0.47 (0.24−0.92)	1.31×10^{-2}
12-*S*-hydroxyeicosatetraenoic acid	0.47 (0.24−0.91)	1.37×10^{-2}
$C_{14}H_{22}O_3$	0.49 (0.25−0.96)	2.08×10^{-2}
2-methyl-3-hydroxy-4-carboxy-5-hydroxymethylpyridine	0.49 (0.25−0.95)	2.39×10^{-2}
2-(4-hydroxy-3-methoxyphenyl) ethanal	2.03 (1.05−3.93)	2.40×10^{-2}
(2-dodecen-1-yl) succinic anhydride	0.51 (0.26−1.00)	2.96×10^{-2}
3-hydroxyisovalerate	1.96 (1.02−3.78)	3.45×10^{-2}
fucose	0.51 (0.27−0.98)	3.60×10^{-2}
6-*O*-phosphono-α-D-glucopyranose	0.53 (0.27−1.01)	4.19×10^{-2}
cadaverine	0.53 (0.27−1.02)	4.29×10^{-2}
2-tetradecenoic acid	0.54 (0.28−1.04)	4.57×10^{-2}

Metabolic Profiles Related to the Radiotherapy

We aimed to find the metabolic alterations that correlated with the radiotherapy treatment course. The ideal sample set should include all four sampling points for each patient; however, only 126 serum samples were collected due to loss of follow-up. Of the 54 lung cancer cases, a matched set of TP1−TP3 was available for 21 patients.

To observe the response after radiotherapy, classification models were performed with 21 patients with TP1−TP3 samples to reveal the metabolic profile changes. Based on ANOVA analysis, Figure 2A demonstrates the changes of the top 25 metabolites differentially expressed at the first three time points. Hierarchical cluster analysis divides these 25 metabolites into two major clusters (Figure 2A, clusters 1 and cluster 2). The averaged trends of clusters 1 and 2 by time points are shown in Figure 2B, which represents the upregulated and downregulated metabolite groups after the initiation of radiation treatment separately. Nine metabolites out of 13 from cluster 1 increased substantially at TP2 and then started to return to baseline levels. While in cluster 2, nine metabolites out of 12 remained below baseline levels during the radiation treatment period.

A 3-dimensional PLS-DA model was also established to demonstrate how the metabolic profile changed over time in these 21 patients. As shown in Figure 3A, the red, green, and blue dots show the classification of the samples into preradiotherapy, one-third of radiotherapy, or two-thirds of radiotherapy, respectively, based on the first three components of PLS-DA. A steady drift of overall metabolic profiles across the duration of radiation treatment was observed in the PLS-DA plot from the start to the end of treatment (TP1 to TP3). The metabolite profiles derived from this subset of patients suggested that serum metabolomics was associated with the responses of RT treatment, which has the potential to be used for the assessment of acute/late toxicity of RT treatment. Volcano plots (Figure 3B,C) were used to identify the most significant metabolites contributing to the classification of the first 3 time points. Among them, nicotinamide and hypoxanthine showed consistent downregulation during the

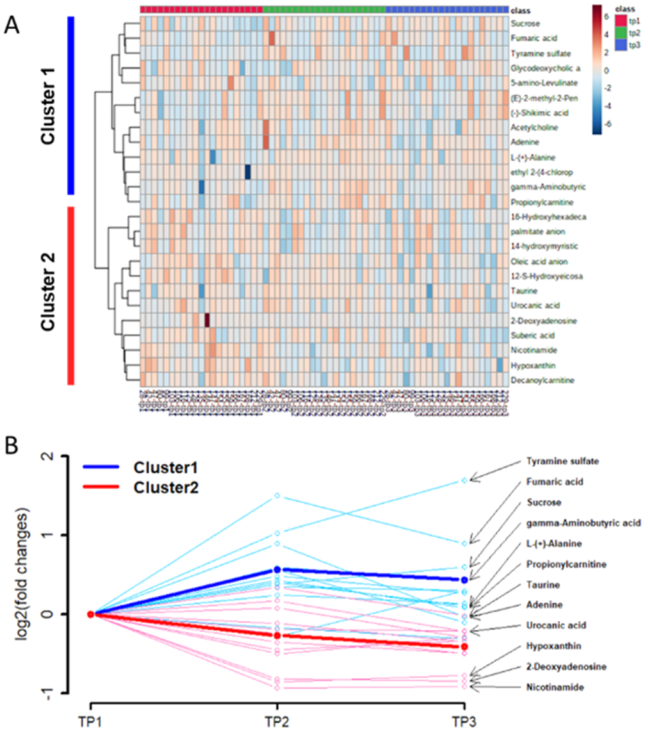

Figure 2. Alterations in the overall serum metabolite profiles during radiation treatment. (A) ANOVA analysis from 21 individuals across the first three time points revealed the top 25 differentially expressed serum metabolites. (B) Two metabolic clusters' dynamics during RT treatment.

sessions of radiotherapy compared with their levels before RT treatment.

Additionally, seven common metabolites were significantly altered (t-test p-value < 0.05) in both TP2 and TP3 by analyzing the subset of the 21-patient cohort. The levels of all these metabolites showed substantial changes in TP2 but started to return to baseline (still significant) in TP3 (Figure 4A). Furthermore, the changing patterns of these 7 metabolites

https://doi.org/10.1021/acs.jproteome.4c00529
J. Proteome Res. 2025, 24, 1662−1671

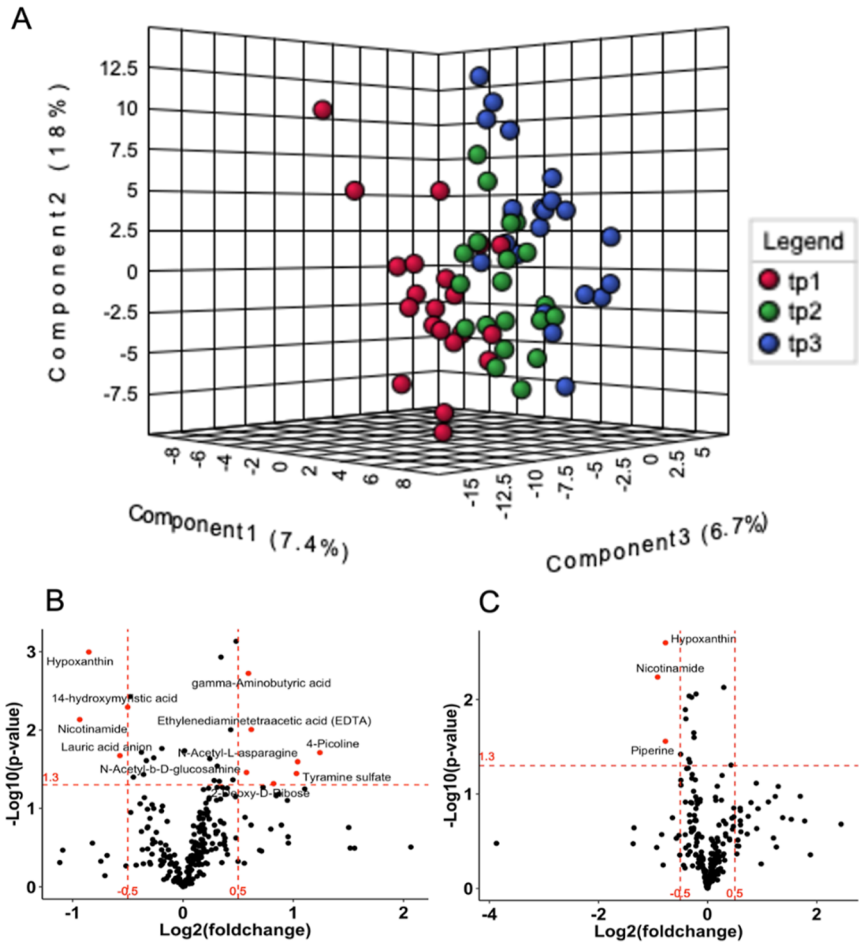

Figure 3. Metabolic trajectory was determined by PLS-DA analysis ($N = 21$). (A) Three-dimensional PLS-DA plot for the initial three time points. (B) The volcano plot illustrated the metabolic dysregulations that occurred in 21 NSCLC cases between TP1 and TP2. (C) The volcano plots illustrated the metabolic dysregulations among 21 NSCLC cases between TP1 and TP3.

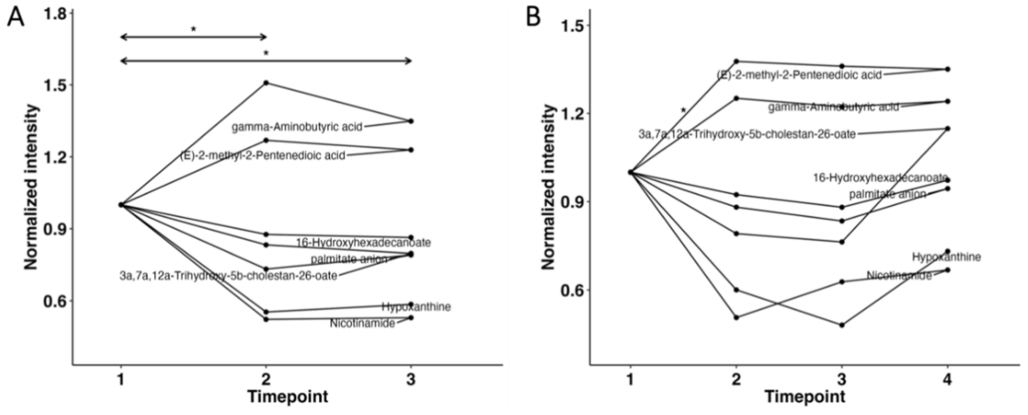

Figure 4. Identification of differentially expressed metabolites related to RT responses. (A) Changing trends of the significant metabolite average for 21 patients by the first 3 time points. (B) Changing trends of the average of the same metabolites for 6 patients from TP1 to TP4.

were plotted in 6 patients with all 4 time points shown in Figure 4B, which was consistent with our findings in the large cohort of NSCLC patients.

Longitudinal Evaluation of Serum Metabolic Changes Perturbed by the Radiotherapy

After investigating the subset of samples from patients with multiple samples collected in the study, we also performed an analysis of all samples to see whether we could generalize our findings from the above analyses. After all, a total of 126 human serum samples from 54 patients were available for this study, which included 47 TP1 samples, 33 TP2 samples, 33 TP3 samples, and 13 TP4 samples. Similarly, supervised multivariable PLS-DA analysis was applied to the acquired LCMS data, and variable importance projection (VIP) analysis determined a group of top-rank metabolites that were perturbed by radiotherapy intervention and indicated the treatment response. Metabolites in serum represent the

https://doi.org/10.1021/acs.jproteome.4c00529
J. Proteome Res. 2025, 24, 1662−1671

Table 3. List of Significantly Altered Metabolites among 4 Time Points[a]

class	compound	fold change					VIP				
		TP2/TP1	TP3/TP1	TP4/TP1	TP3/TP2	TP4/TP3	TP1 vs TP2	TP1 vs TP3	TP1 vs TP4	TP2 vs TP3	TP3 vs TP4
fatty acids	(*E*)-2-methyl-2-pentenedioic acid	1.20	1.27	1.19	1.06	0.93	1.91	2.36*	1.39	0.8	0.62
	sebacic acid	1.13	0.80	1.19	0.70	1.49	1.18	0.85	1.18	2.42*	2.07
	10-hydroxydecanoic acid	0.76	1.11	1.24	1.46	1.12	2.45*	0.53	1.39	1.74	1.44
	(9*E*,11*E*)-13-hydroperoxy-9,11-octadecadienoic acid	0.79	0.96	1.38	1.22	1.44	1.86*	0.01	1.06	2.37	1.16
	dibutyl decanedioate	0.76	0.84	1.41	1.10	1.68	2.4*	1.42	0.84	1.07	1.95
	(5*Z*,8*Z*,11*Z*,14*Z*)-5,8,11,14-icosatetraenoate	0.79	0.81	0.74	1.03	0.91	2.3*	1.95	2.3	0.09	0.67
	docosahexaenoic acid	0.70	0.66	0.75	0.94	1.14	2.1	1.89*	1.03	0.22	0.59
	(−)-12(*R*),13(*S*)-vernolic acid	0.72	0.79	1.50	1.10	1.89	2.21*	1.62	0.61	0.36	1.83
	16-hydroxyhexadecanoate	0.88	0.87	0.91	1.00	1.04	2.09*	1.98*	1.09	0.01	0.63
	lauric acid	0.67	1.02	0.87	1.52	0.85	2.29*	1.39	0.04	0.51	1.21
	leucic acid	0.95	0.90	0.76	0.95	0.84	0.43	0.31	1.55*	0.18	1.9
	suberic acid	1.13	0.80	1.19	0.87	1.21	1.18	0.85	1.18	2.42*	2.07
carboxylic acids and derivatives	γ-aminobutyric acid	1.26	1.25	1.03	0.99	0.83	1.88*	1.61*	0.66	0.13	0.88
	fumaric acid	1.99	1.89	1.58	0.95	0.84	1.6	2.37*	2.45	0.95	0.15
	DL-homocysteine	0.95	0.82	1.07	0.87	1.31	0.48	1.46*	0.69	1.31	2.15
	2-amino-3-ketobutyric acid	0.83	0.67	0.82	0.81	1.23	1.35	1.61*	0.7	0.4	0.7
organic sulfuric acids and derivatives	tyramine sulfate	1.06	2.91	1.23	2.75	0.42	1.2	1.9*	1.19	1.31	0.6
	acesulfame	0.81	0.70	0.09	0.86	0.12	0.21	1.03	2.1*	1.11	1.43
benzene and substituted derivatives	4-dodecylbenzenesulfonic acid	0.73	0.67	0.83	0.92	1.24	2.19	2.49*	1.17	0.72	1
pyridines and derivatives	nicotinamide	0.43	0.41	0.48	0.95	1.19	3.84*	3.97*	2.24**	1.34	1.73
prenol lipids	perillic acid	0.78	0.89	1.08	1.15	1.21	1.31*	0.55	0.71	0.96	1.41
imidazopyrimidines	hypoxanthine	0.56	0.64	0.61	1.14	0.94	3.9**	3.01*	2.11**	0.81	0.69
phenols	homovanillic acid	1.08	1.23	1.19	1.14	0.97	0.98	2.28*	1.02	1.78	0.72

[a] *p-value < 0.05. **p-value < 0.01. ***p-value < 0.001.

https://doi.org/10.1021/acs.jproteome.4c00529
J. Proteome Res. 2025, 24, 1662−1671

combined metabolomes between normal tissues and malignant cells, which can reflect many important physiological homeostases such as glucose metabolism, DNA damage/repair, and oxidative stress in these irradiated cells.

Twenty-three metabolites (9.1%) achieved statistical significance from both multivariate (PLS-DA VIP selection) and univariate analyses (fold-change), including 21 from negative ion mode and 2 from positive ion mode (Table 3). The fold changes were calculated by dividing the average intensities of the other three time points, respectively, by that of the first time point. Most of the differentially expressed metabolites did not show monotonous changes, and the turning points emerged between the third and fourth time points, which was consistent with the recovery period after radiation therapy.

Notably, over half of the metabolites (12/23) were classified as fatty acids, and except for (*E*)-2-methyl-2-pentenedioic acid, all other serum lipid metabolites showed reduced levels in serum after the initiation of radiation treatment, which suggested that lipid metabolism can be used for monitoring cancer treatment response. Four carboxylic acids exhibited immediate responses to radiation treatment in the longitudinal analysis. The serum concentrations of these carboxylic acids rapidly returned to or close to physiological levels at the first follow-up visit. We identified several metabolites associated with dietary items, such as food, beverages, and supplements. For example, docosahexaenoic acid (DHA) is commonly found in fish oil, which displayed a continuous descent. DHA is one of the supplements for radiation therapy, which has been shown to improve the efficacy of first-line chemotherapy in patients with advanced NSCLC.[23]

DISCUSSION

It is now well recognized that untargeted metabolomics can rapidly screen the highly abundant metabolites in human biofluids, such as blood, urine, and cerebrospinal fluid, for biomarker discoveries and disease mechanism studies. To investigate the longitudinal changes in small molecules in NSCLC patients receiving external beam radiotherapy, we employed untargeted metabolomics to examine the serum samples collected at the Ohio State University Medical Center.

In this study, we found that several fatty acid species, including long-, medium-, and short-chain fatty acids, were deregulated at the initiation of radiotherapy. Two long-chain fatty acids (9*E*,11*E*)-13-hydroperoxy-9,11-octadecadienoic acid and (5*Z*,8*Z*,11*Z*,14*Z*)-5,8,11,14-icosatetraenoate were down-regulated after radiation treatment started. (5*Z*,8*Z*,11*Z*,14*Z*)-5,8,11,14-Icosatetraenoate or called arachidonic acid is a long-chain fatty acid anion derived from the arachidonic acid. It has been found that arachidonic acid and eicosanoid synthesis by glomeruli after a single dose of 9.5 Gy radiation can provoke the cyclooxygenase (COX) activity, further increasing the radiation-induced albumin permeability in the kidney.[27] Thus, radiotherapy potentially changes the biological equilibrium of arachidonic acid metabolism, further modulating inflammation and immunity with other PUFA molecules.[28] Meanwhile, (9*E*,11*E*)-13-hydroperoxy-9,11-octadecadienoic acid is a hydroperoxy polyunsaturated fatty acid from a group of organic compounds known as linoleic acids and derivatives, and the decreased concentrations of linoleic acid (C18:2) were previously observed in breast cancer patients as compared to controls.[29] Several medium- and short-chain fatty acids were also significantly impacted by radiation treatment in our study and are in agreement with some earlier reports.[30] One recent study investigated the pre- and post-RT serum samples of a cohort of head and neck cancer patients using gas chromatography−mass spectrometry. Similar to our results, this study found that the serum level of sebacic acid was increased 1.79-fold in the post-RT samples.[31] Furthermore, metabolic therapies such as ketogenic diets have indicated a potential for improving radiotherapy responses and outcomes in cancer patients in small clinical trials.[32]

It is known that carbohydrate metabolism is critical for cancer progression. As the hub of glucose and lipid metabolism, the activities of the TCA cycle are decisive factors for the outcome of cancer treatment. Particularly, fumaric acid, a critical component of the TCA cycle, was found to be upregulated during radiation treatment in this study. Accumulation of fumaric acid is essential for cell proliferation and survival and confers resistance to radiation-induced DNA damages by promoting early mitotic entry and suppressing checkpoint maintenance.[33] Consistently, the upregulation of fumaric acid and γ-aminobutyric acid (GABA) promotes the metabolism of nonessential amino acids and provides additional energy sources and nitrogen donors for tissue recovery damaged by chemoradiation therapy. Furthermore, the secretion of GABA is a potential protective mechanism that alleviates radiation-induced oxidative stress and promotes cell proliferation.[34]

Furthermore, RNA and DNA synthesis-related metabolites were also identified in our samples. Radiotherapy resistance may be related to nicotinamide *N*-methyltransferase (NNMT) overexpression.[35] Higher NNMT can enhance the radiation resistance of cells by depleting niacinamide.[36] Hypoxanthine has been reported as a biomarker of urine and serum exposure to ionizing radiation in both nonhuman primates[37] and humans.[38] In purine metabolism, hypoxanthine can be converted to xanthine and uric acid by xanthine oxidase, which mediates reactive oxygen species (ROS) production and promotes cell apoptosis.[39] Although the levels of xanthine and uric acid in this study did not show significant changes, it is plausible that radiotherapy induces a metabolic shift, leading to an increased consumption of hypoxanthine. This shift may occur without a corresponding accumulation of downstream metabolites as the system can regulate their levels through various compensatory mechanisms, such as enhanced excretion or utilization in other pathways.

Radio- and chemotherapy produce highly reactive oxygen species (ROS) that induce DNA damage during treatment, and several serum metabolites identified in this study are related to the modulation of ROS pathways. Therefore, we hypothesize that the increase in these serum metabolites can also be a result of the upregulation of ROS production.[26] For example, tyramine belongs to the tyrosine metabolic pathway and is excreted in the urine. When phenylalanine is hydroxylated by hydroxyl radicals, the hydroxylated product, tyrosine, is increased, indicating a high rate of protein oxidative damage. Therefore, elevated tyramine levels, as indicated in our study and consistent with other research results,[40] may be a way for the human body to eliminate excess tyrosine produced after ionizing radiation exposure. Similarly, homocysteine, as one of the significantly changed metabolites over the duration of the treatment, has been reported to activate caspase-9 and caspase-3 to induce apoptosis. The increase in ROS also activates the PI3K/AKT pathway, which is highly expressed by serine/threonine kinase (AKT) and consumes a large amount of threonine. As a downstream product of threonine, 2-amino-3-

https://doi.org/10.1021/acs.jproteome.4c00529
J. Proteome Res. 2025, 24, 1662−1671

ketobutyric acid is also downregulated accordingly.[41] Together, a subset of these altered serum metabolites are indicators of the formation of intracellular ROS and activation of pro-inflammatory responses.[42]

Several metabolites are commonly found to be elevated in tumors, including lactate, choline-containing compounds, nucleosides, myoinositol, and lipids.[43,44] The interplay between lung cancer cells and the immunologic microenvironment orchestrates the alterations of a wide variety of biomolecules responding to the radiation treatment.[45] In order to predict serious adverse events, it is necessary to identify biomolecules and associated metabolic pathways altered at an early stage of RT-induced tissue damage through noninvasive or minimum-invasive procedures. The biomarkers capable of predicting pulmonary complications would be a significant step toward minimizing the incidence and severity of these complications.[46]

CONCLUSIONS

To the best of our knowledge, our study is the first to longitudinally investigate the serum metabolomics in response to external beam thoracic radiation treatment. The metabolites identified in this study are primarily categorized as lipids, amino acids, and nucleic acids. These metabolites have been found to be highly associated with the biochemical and molecular reprogramming during lung tumorigenesis.[47] Meanwhile, there are a few limitations of this study. First, due to the lack of commercially available chemical standards, some of our reported metabolites cannot be fully and confidently annotated for downstream investigations. Second, because of the limitation of cohort size, these identified biomarkers need to be validated further in in vivo models and separate cohorts. Lastly, the initiation of metastatic NSCLC cancer, which is highly resistant to standard treatments, is a complex phenomenon influenced by the genetic characteristics of lung cancer cells.

ASSOCIATED CONTENT

Data Availability Statement

The mass spectra data have been deposited in the MassIVE database (https://massive.ucsd.edu/ProteoSAFe/static/massive.jsp) with access # MSV000096105.

Supporting Information

The Supporting Information is available free of charge at https://pubs.acs.org/doi/10.1021/acs.jproteome.4c00529.

> Serum sample preparation; methods on the HPLC-Q-Exactive mass spectrometer system; data quality control and assessment; statistical analyses according to timeline and symptomatic situation; integral dose evaluation; detailed demographic information; internal standards list and the concentration; differential metabolites associated with brain metastasis before radiation treatment; metabolites associated with two metabolic clusters' dynamics during RT treatment; supplementary table for Figure 4A; supplementary table for Figure 4B; characteristics of each metabolite identified in the LC−MS experiment; PCA plot of the biological sample (BS), pooled QC sample, and human serum QC (HSQC) sample; and metabolic feature selection (PDF)

AUTHOR INFORMATION

Corresponding Authors

Jiangjiang Zhu − *Department of Human Sciences, The Ohio State University, Columbus, Ohio 43210, United States;* orcid.org/0000-0002-4548-8949; Email: zhu.2484@osu.edu

Arnab Chakravarti − *Department of Radiation Oncology, The Ohio State University, Columbus, Ohio 43210, United States;* orcid.org/0000-0002-5392-8721; Email: chakravarti.7@osu.edu, Arnab.Chakravarti@osumc.edu

Authors

Wei Meng − *Department of Radiation Oncology, The Ohio State University, Columbus, Ohio 43210, United States*

Rui Xu − *Department of Human Sciences, The Ohio State University, Columbus, Ohio 43210, United States*

Eric Miller − *Department of Radiation Oncology, The Ohio State University, Columbus, Ohio 43210, United States*

Xiaowei Sun − *Department of Human Sciences, The Ohio State University, Columbus, Ohio 43210, United States*

Jennifer Thurmond − *Department of Radiation Oncology, The Ohio State University, Columbus, Ohio 43210, United States*

Amy Webb − *Center for Biostatistics, The Ohio State University, Columbus, Ohio 43210, United States*

Joseph McElroy − *Center for Biostatistics, The Ohio State University, Columbus, Ohio 43210, United States*

Joshua Palmer − *Department of Radiation Oncology, The Ohio State University, Columbus, Ohio 43210, United States*

Dominic J. DiCostanzo − *Department of Radiation Oncology, The Ohio State University, Columbus, Ohio 43210, United States*

Shiqi Zhang − *Department of Human Sciences, The Ohio State University, Columbus, Ohio 43210, United States*

Hisashi Yamaguchi − *Department of Radiation Oncology, The Ohio State University, Columbus, Ohio 43210, United States*

Saikh Jaharul Haque − *Department of Radiation Oncology, The Ohio State University, Columbus, Ohio 43210, United States*

Complete contact information is available at: https://pubs.acs.org/10.1021/acs.jproteome.4c00529

Author Contributions

‖W.M. and R.X. contributed equally to this work.

Notes

The authors declare the following competing financial interest(s): J.P.: Huron Consulting Group, consultant; Nococure, Advisory Board; Kroger, grant funding; More Health, consultant; DePuy Synthes, speaking fees; NCCN Pediatric Brain Tumors, member; NCI/NIH grant support R01, R702; Genentech, research; Varian medical systems, speaking fees; ICOTEC, speaking fees. All other authors declare that they have no conflicts of interest.

REFERENCES

(1) Huang, J.; Deng, Y.; Tin, M. S.; et al. Distribution, Risk Factors, and Temporal Trends for Lung Cancer Incidence and Mortality: A Global Analysis. *Chest* **2022**, *161* (4), 1101−1111.

(2) Siegel, R. L.; Miller, K. D.; Fuchs, H. E.; Jemal, A. Cancer statistics, 2022. *Ca-Cancer J. Clin.* **2022**, *72* (1), 7−33.

https://doi.org/10.1021/acs.jproteome.4c00529
J. Proteome Res. 2025, 24, 1662−1671

(3) Ridge, C. A.; McErlean, A. M.; Ginsberg, M. S. *Epidemiology of Lung Cancer*; Thieme Medical Publishers, 2013; Vol. *30*, pp 93−98.
(4) Molina, J. R.; Yang, P.; Cassivi, S. D.; Schild, S. E.; Adjei, A. A. *Non-small Cell Lung Cancer: Epidemiology, Risk Factors, Treatment, and Survivorship*; Elsevier, 2008; pp 584−594.
(5) Curran, W. J.; Paulus, R.; Langer, C. J.; et al. Sequential vs. concurrent chemoradiation for stage III non-small cell lung cancer: randomized phase III trial RTOG 9410. *J. Natl. Cancer Inst.* **2011**, *103* (19), 1452−1460.
(6) Timmerman, R.; Papiez, L.; McGarry, R.; et al. Extracranial stereotactic radioablation: results of a phase I study in medically inoperable stage I non-small cell lung cancer. *Chest* **2003**, *124* (5), 1946−1955.
(7) Ginsberg, R. J.; Rubinstein, L. V. Randomized trial of lobectomy versus limited resection for T1 N0 non-small cell lung cancer. Lung Cancer Study Group. *Ann. Thorac. Surg.* **1995**, *60* (3), 615−622.
(8) Hanania, A. N.; Mainwaring, W.; Ghebre, Y. T.; Hanania, N. A.; Ludwig, M. Radiation-Induced Lung Injury: Assessment and Management. *Chest* **2019**, *156* (1), 150−162.
(9) Loo, B. W. Stereotactic ablative radiotherapy (SABR) for lung cancer: What does the future hold? *Ann. Thorac. Surg.* **2011**, *3* (3), 150−152.
(10) Hanahan, D.; Weinberg, R. A. Hallmarks of cancer: the next generation. *Cell* **2011**, *144* (5), 646−674.
(11) Warburg, O.; Wind, F.; Negelein, E. The metabolism of tumors in the body. *J. Gen. Physiol.* **1927**, *8* (6), 519−530.
(12) Maeda, J.; Higashiyama, M.; Imaizumi, A.; et al. Possibility of multivariate function composed of plasma amino acid profiles as a novel screening index for non-small cell lung cancer: a case control study. *BMC Cancer* **2010**, *10*, 690.
(13) Ferreira, M. R.; Sands, C. J.; Li, J. V.; Andreyev, J. N.; Chekmeneva, E.; Gulliford, S.; Marchesi, J.; Lewis, M. R.; Dearnaley, D. P. Impact of pelvic radiation therapy for prostate cancer on global metabolic profiles and microbiota-driven gastrointestinal late side effects: a longitudinal observational study. *Int. J. Radiat. Oncol. Biol. Phys.* **2021**, *111* (5), 1204−1213.
(14) Schelli, K.; Rutowski, J.; Roubidoux, J.; Zhu, J. Staphylococcus aureus methicillin resistance detected by HPLC-MS/MS targeted metabolic profiling. *J. Chromatogr. B* **2017**, *1047*, 124−130.
(15) Mistrik, R. *mzCLOUD: A Spectral Tree Library for the Identification of Unknown*; American Chemical Society: 1155 16th Street, NW, Washington, DC 20036 USA, 2018.
(16) Hofestädt, R., Freier, A., Höding, M., Lange, M., Scholz, U.. Molecular Database Integration: Analysis of Metabolic Network Control. *Proceedings of the First International Conference on Bioinformatics of Genome Regulation and Structure (BGRS'98)*, 1998.
(17) Ayers, M. *ChemSpider: The Free Chemical Database*, 2012.
(18) Zhang, S.; Xu, M.; Sun, X.; et al. Black raspberry extract shifted gut microbe diversity and their metabolic landscape in a human colonic model. *J. Chromatogr. B:Anal. Technol. Biomed. Life Sci.* **2022**, *1188*, 123027.
(19) Zou, H.; Hastie, T. Regularization and variable selection via the elastic net. *J. Roy. Stat. Soc. B Stat. Methodol.* **2005**, *67* (2), 301−320.
(20) Tibshirani, R. Regression Shrinkage and Selection Via the Lasso. *J. Roy. Stat. Soc. B* **1996**, *58* (1), 267−288.
(21) Tesselaar, M. E.; Osanto, S. Risk of venous thromboembolism in lung cancer. *Curr. Opin. Pulm. Med.* **2007**, *13* (5), 362−367.
(22) Zhang, M.; Wu, S.; Hu, C. Do lung cancer patients require routine anticoagulation treatment? A meta-analysis. *J. Int. Med. Res.* **2020**, *48* (1), 300060519896919.
(23) Murphy, R. A.; Mourtzakis, M.; Chu, Q. S.; Baracos, V. E.; Reiman, T.; Mazurak, V. C. Supplementation with fish oil increases first-line chemotherapy efficacy in patients with advanced nonsmall cell lung cancer. *Cancer* **2011**, *117* (16), 3774−3780.
(24) Ali, A.; Goffin, J. R.; Arnold, A.; Ellis, P. M. Survival of patients with non-small-cell lung cancer after a diagnosis of brain metastases. *Curr. Oncol.* **2013**, *20* (4), e300−e306.
(25) Sperduto, P. W.; Yang, T. J.; Beal, K.; et al. Estimating Survival in Patients With Lung Cancer and Brain Metastases: An Update of the Graded Prognostic Assessment for Lung Cancer Using Molecular Markers (Lung-molGPA). *JAMA Oncol.* **2017**, *3* (6), 827−831.
(26) Vettore, L.; Westbrook, R. L.; Tennant, D. A. New aspects of amino acid metabolism in cancer. *Br. J. Cancer* **2020**, *122* (2), 150−156.
(27) Sharma, M.; McCarthy, E. T.; Sharma, R.; et al. Arachidonic acid metabolites mediate the radiation-induced increase in glomerular albumin permeability. *Exp. Biol. Med.* **2006**, *231* (1), 99−106.
(28) Shaikh, S.; Channa, N. A.; Talpur, F. N.; Younis, M.; Tabassum, N. Radiotherapy improves serum fatty acids and lipid profile in breast cancer. *Lipids Health Dis.* **2017**, *16* (1), 92−98.
(29) Shaikh, S.; Channa, N. A.; Talpur, F. N.; Younis, M.; Tabassum, N. Radiotherapy improves serum fatty acids and lipid profile in breast cancer. *Lipids Health Dis.* **2017**, *16* (1), 92.
(30) Hoffer, L. J.; Taveroff, A.; Robitaille, L.; Mamer, O. A.; Reimer, M. L. α-Keto and α-hydroxy branched-chain acid interrelationships in normal humans. *J. Nutr.* **1993**, *123* (9), 1513−1521.
(31) Roś-Mazurczyk, M.; Wojakowska, A.; Marczak, Ł.; et al. Ionizing radiation induces changes in profile of metabolites in serum of cancer patients. *Acta Biochim. Pol.* **2017**, *64* (1), 189−193.
(32) Oliveira, C. L.; Mattingly, S.; Schirrmacher, R.; Sawyer, M. B.; Fine, E. J.; Prado, C. M. A nutritional perspective of ketogenic diet in cancer: a narrative review. *J. Acad. Nutr. Diet.* **2018**, *118* (4), 668−688.
(33) Johnson, T. I.; Costa, A. S.; Ferguson, A. N.; Frezza, C. Fumarate hydratase loss promotes mitotic entry in the presence of DNA damage after ionising radiation. *Cell Death Dis.* **2018**, *9* (9), 913.
(34) Abd El-Hady, A. M.; Gewefel, H. S.; Badawi, M. A.; Eltahawy, N. A. Gamma-aminobutyric acid ameliorates gamma rays-induced oxidative stress in the small intestine of rats. *J. Basic Appl. Zool.* **2017**, *78* (1), 2.
(35) Sartini, D.; Morganti, S.; Guidi, E.; et al. Nicotinamide N-methyltransferase in non-small cell lung cancer: promising results for targeted anti-cancer therapy. *Cell Biochem. Biophys.* **2013**, *67* (3), 865−873.
(36) D'Andrea, F. P.; Safwat, A.; Kassem, M.; Gautier, L.; Overgaard, J.; Horsman, M. R. Cancer stem cell overexpression of nicotinamide N-methyltransferase enhances cellular radiation resistance. *Radiother. Oncol.* **2011**, *99* (3), 373−378.
(37) Johnson, C. H.; Patterson, A. D.; Krausz, K. W.; et al. Radiation metabolomics. 5. Identification of urinary biomarkers of ionizing radiation exposure in nonhuman primates by mass spectrometry-based metabolomics. *Radiat. Res.* **2012**, *178* (4), 328−340.
(38) Kim, K.; Yeo, S.-G.; Yoo, B. C. Identification of hypoxanthine and phosphoenolpyruvic Acid as serum markers of chemoradiotherapy response in locally advanced rectal cancer. *Cancer Treat Res.* **2015**, *47* (1), 78.
(39) Kim, Y.-J.; Ryu, H.-M.; Choi, J.-Y.; et al. Hypoxanthine causes endothelial dysfunction through oxidative stress-induced apoptosis. *Biochem. Biophys. Res. Commun.* **2017**, *482* (4), 821−827.
(40) Orhan, H.; Vermeulen, N. P.; Tump, C.; Zappey, H.; Meerman, J. H. Simultaneous determination of tyrosine, phenylalanine and deoxyguanosine oxidation products by liquid chromatography-tandem mass spectrometry as non-invasive biomarkers for oxidative damage. *J. Chromatogr. B* **2004**, *799* (2), 245−254.
(41) Debabov, V. G. The threonine story. *Microbial Production of l-Amino Acids*; Springer, 2003; pp 113−136.
(42) Kim, D. J.; Koh, J.-M.; Lee, O.; et al. Homocysteine enhances apoptosis in human bone marrow stromal cells. *Bone* **2006**, *39* (3), 582−590.
(43) Griffin, J. L.; Shockcor, J. P. Metabolic profiles of cancer cells. Research Support, Non-U.S. Gov't Review. *Nat. Rev. Cancer* **2004**, *4* (7), 551−561.
(44) Noch, E.; Khalili, K. Molecular mechanisms of necrosis in glioblastoma: the role of glutamate excitotoxicity. Research Support, N.I.H., Extramural Review. *Cancer Biol. Ther.* **2009**, *8* (19), 1791−1797.

https://doi.org/10.1021/acs.jproteome.4c00529
J. Proteome Res. 2025, 24, 1662−1671

(45) Tsoutsou, P. G.; Koukourakis, M. I. Radiation pneumonitis and fibrosis: mechanisms underlying its pathogenesis and implications for future research. *Int. J. Radiat. Oncol. Biol. Phys.* **2006**, *66* (5), 1281−1293.
(46) Provatopoulou, X.; Athanasiou, E.; Gounaris, A. Predictive markers of radiation pneumonitis. *Anticancer Res.* **2008**, *28* (4C), 2421−2432.
(47) Fahrmann, J. F.; Grapov, D. D.; Wanichthanarak, K.; DeFelice, B. C.; Salemi, M. R.; Rom, W. N.; Gandara, D. R.; Phinney, B. S.; Fiehn, O.; Pass, H.; et al. Integrated Metabolomics and Proteomics Highlight Altered Nicotinamide- and Polyamine Pathways in Lung Adenocarcinoma. *Carcinogenesis* **2017**, *38* (3), bgw205−bgw280.

https://doi.org/10.1021/acs.jproteome.4c00529
J. Proteome Res. 2025, 24, 1662−1671